JOURNAL OF SOLID STATE CHEMISTRY 97, 141–149 (1992)

Electrical Conductivity of New Me_2SO_4 (Me = Na, K, and Rb) Added to Li_2SO_4-Li_2CO_3 Eutectic Composite Material

K. SINGH and S. S. BHOGA

Department of Physics, Nagpur University, Nagpur-440010, India

Received June 21, 1991; in revised form September 11, 1991

A systematic study on electrical conductivity of new Me_2SO_4 (Me = Na, K, and Rb) added to Li_2SO_4-Li_2CO_3 eutectic composite materials has been carried out. This addition showed two maxima in the conductivity isotherm for the entire impurity concentration range investigated (0 to 8 mole%). The first maximum in conductivity at 1 mole% of Me_2SO_4 has been discussed in the light of lattice distortion resulting from the formation of solid solution. The second maximum at 5 mole% of Me_2SO_4 (Me = Na, K, and Rb) has been explained using dispersed phase theory. The results are substantiated by XRD, DTA, and microstructural morphology (SEM).

Introduction

With the discovery of composite electrolytes, a new field in solid state electrochemistry was started by Liang (*1*) in 1973. Composite electrolytes are heterogeneous solid systems. Poulsen (*2*) has provided an excellent review on composite electrolytes. In this area, ionic conductivity has been the only parameter which at present is the subject of optimization.

A number of homovalent binary systems have been reported to show conductivity enhancement. It is reported that the highest conductivity for a composition belonging to any binary system may be correlated with the amount of eutectic and/or fine grained solid solution material formed during the solidification of the mixture (*2*). This particular fact inspired the present study on the $60Li_2SO_4:40Li_2CO_3$ eutectic, where the phases corresponding to Na_2SO_4, K_2SO_4, and Rb_2SO_4 have been purposefully added to enhance the conductivity of the resulted composite electrolytes.

The phase diagram study of the $Li_2SO_4:Li_2CO_3$ binary system reveals the presence of a eutectic composition at 60–40 mole% (*3, 4*). It has been reported by Deshpande and Singh (*5*) that the eutectic composition gives maximum conductivity in the entire binary system. Further, an enhancement in the conductivity of this eutectic has been observed by addition of LiX (X = F, Cl, Br, and I) and Na_2SO_4 (*6, 7*). On the other hand, addition of a number of divalent sulphates reduces the conductivity (*8*).

Experimental

The initial ingredients, Li_2SO_4, Me_2SO_4 with purity greater than 99.9%, were procurred from Fluka AG, Germany, and E. Merck, Darmstadt. The Me_2SO_4 were added to the $Li_2SO_4:Li_2CO_3$ eutectic by keeping constant its 60:40 mole ratio. The mode of sample preparation and conductivity measurement were similar to those discussed earlier (*8, 9*). The prepared samples were characterized by X-ray powder dif-

0022-4596/92 $3.00

fraction (XRD) using Cu$K\alpha$ radiation and differential thermal analysis (DTA). The microstructures were examined with a Cambridge 250 Mark-III scanning electron microscope (SEM).

Results and Discussion

Conductivity behavior of composite solid electrolytes can be better understood through the knowledge of X-ray powder diffraction results obtained toward the range of solid solubility and the possibility of intermediate phase formation.

The X-ray powder diffraction patterns of all compositions showed a slight potential line broadening in general; particularly in the 2θ range from 60° to 90° it is more prominent. It is also seen that such a line broadening is large for (i) quenched samples and (ii) multi-component (more than two phases) systems. The potential line broadening is attributed to: (a) further reduction in the grain size (eutectic composition showed minimum grain size in the entire binary system) resulting from the quenching and (b) the composite nature of the samples under investigation. Thus for meaningful discussion, the lines of higher angles (>60°) are not taken into consideration for further analysis. A comparison of X-ray diffraction data (a few lines as indicative) with JCPDS values listed in Tables I–III shows that up to 1.5 mole% of Na_2SO_4, K_2SO_4, and Rb_2SO_4 no intermediate phases corresponding to $LiNaSO_4$, $LiKSO_4$, and $LiRbSO_4$ form in the respective systems. Also, the absence of peaks related to Na_2SO_4, K_2SO_4, and Rb_2SO_4 rules out the possibility of precipitation or separation of these phases in the eutectic matrix.

In the present case, Na_2SO_4, K_2SO_4, and Rb_2SO_4 are the participating intermediate phases, which also must have limited solubilities for the neighboring phase. Thus, in order to check the possibility of limited solid solubility, lattice parameters of Li_2SO_4 are calculated. Since experimental errors in the measurement of d values are small (0.001 Å) in the 2θ range from 30°–60°, only those lines appearing in this range are selected for the calculation of the lattice

TABLE I

COMPARISON OF d AND I/I_0 WITH THOSE OF JCPDS DATA FOR Na_2SO_4 ADDED EUTECTIC

1.5 mole%			3 mole%			5 mole%		
d_{obs}/d_{ASTM}	I_{obs}/I_{ASTM}	Phase	d_{obs}/d_{ASTM}	I_{obs}/I_{ASTM}	Phase	d_{obs}/d_{ASTM}	I_{obs}/I_{ASTM}	Phase
4.02/4.03	76/100	LS	4.16/4.16	21/85	LC	4.16/4.16	21/85	LC
3.99/3.99	100/100	LS	4.13/4.13	15/95	LS	4.16/4.16	19/85	LC
3.84/3.84	7/20	LC	4.02/4.04	89/100	LS	3.99/4.00	100/100	LS
3.49/3.49	17/20	LS	3.99/4.00	100/100	LS	3.94/3.91	32/75	LN
2.81/2.81	6/100	LC	3.92/3.92	35/40	LS	3.91/3.91	32/80	LC
2.63/2.62	6/20	LC	3.82/3.81	16/100	LN	3.81/3.81	33/100	LN
2.43/2.43	9/40	LC	3.17/3.18	19/30	LS	3.48/3.48	18/20	LS
2.40/2.40	7/10	LS	3.04/3.03	9/25	LC	3.16/3.16	25/40	LS
1.88/1.86	3/18	LC	3.02/3.02	6/40	LN	3.01/3.02	13/46	LN
1.57/1.56	2/2	LS	2.91/2.91	6/80	LC	2.94/2.94	17/40	LN
1.53/1.52	2/4	LS	2.81/2.81	10/100	LC	2.81/2.81	7/100	LC
1.49/1.49	2/4	LS	2.74/2.74	5/80	LN	2.74/2.74	19/80	LN
1.42/1.42	2/2	LS	2.47/2.47	21/20	LS	2.47/2.47	19/20	LS

Note. LS is Li_2SO_4, LC is Li_2CO_3, and LN is $LiNaSO_4$.

TABLE II

COMPARISON OF d AND I/I_0 WITH THOSE OF JCPDS DATA FOR K_2SO_4 ADDED EUTECTIC

1.5 mole%			3 mole%			5 mole%		
d_{obs}/d_{ASTM}	I_{obs}/I_{ASTM}	Phase	d_{obs}/d_{ASTM}	I_{obs}/I_{ASTM}	Phase	d_{obs}/d_{ASTM}	I_{obs}/I_{ASTM}	Phase
4.15/4.16	75/85	LC	4.15/4.16	18/85	LC	4.16/4.16	16/85	LC
4.02/4.03	77/100	LS	4.02/4.02	72/100	LS	4.02/4.04	72/100	LS
3.99/3.99	100/100	LS	4.00/4.00	100/100	LS	4.00/4.00	100/100	LS
3.92/3.91	31/45	LS	3.96/3.96	38/100	LK	3.96/3.96	59/100	LK
3.80/3.80	2/20	LC	3.92/3.92	34/40	LS	3.92/3.92	26/40	LS
3.48/3.49	17/20	LS	3.80/3.80	6/20	LC	3.48/3.49	15/20	LS
3.18/3.17	19/30	LS	3.48/3.49	17/20	LS	3.17/3.18	18/30	LS
3.16/3.16	31/40	LS	3.16/3.16	25/40	LS	3.13/3.13	12/12	LS
2.92/2.91	4/80	LC	3.10/3.10	21/70	LC	3.09/3.09	33/70	LK
2.82/2.81	6/100	LC	2.91/2.91	6/80	LC	2.91/2.91	8/80	LC
2.79/2.79	9/10	LS	2.81/2.81	8/100	LC	2.79/2.79	9/10	LS
2.4/2.4	5/40	LC	2.57/2.57	9/35	LK	2.57/2.57	16/35	LK
2.40/2.40	7/10	LS	2.41/2.41	8/6	LK	2.47/2.47	19/20	LS
2.27/2.27	1/20	LC	2.40/2.40	10/10	LS	2.46/2.46	14/16	LK

Note. LK is $LiKSO_4$.

cell constants. First of all, the lattice parameters of unquenched and quenched Li_2SO_4 are compared so as to see the effect of quenching (Table IV). It is observed that quenching produces a distortion in the lattice. This can also be seen clearly from the values of the lattice cell constants given in Table IV where, along a and b axes there is a slight change in the 4th and 3rd places, but along c-axis the change is quite prominent (in the 2nd place). From this it evidently can be said that the addition of Me_2SO_4 up to 1.5 mole% gives rise to the formation of substitutional solid solution through the replacement of a fraction of Li^+ (0.6 Å) by Na^+ (0.95 Å), K^+ (1.33 Å), and Rb^+ (1.48 Å). As the ionic sizes of the guest ions are bigger than that of Li^+, in each case, an anisotropic expansion in the lattice

TABLE III

COMPARISON OF d AND I/I_0 WITH THOSE OF JCPDS DATA FOR Rb_2SO_4 ADDED EUTECTIC

1.5 mole%			3 mole%		
d_{obs}/d_{ASTM}	I_{obs}/I_{ASTM}	Phase	d_{obs}/d_{ASTM}	I_{obs}/I_{ASTM}	Phase
4.15/4.16	16/85	LC	4.04/4.04	22/100	LS
4.00/4.04	79/100	LS	3.99/3.99	100/100	LS
3.98/3.99	100/100	LS	3.91/3.91	42/45	LS
3.91/3.92	29/40	LS	3.38/3.38	11/10	LS
3.80/3.80	9/20	LC	3.17/3.17	22/30	LS
3.47/3.49	19/20	LS	3.14/3.11	23/100	RbS
3.38/3.38	8/10	LS	3.03/3.00	10/95	RbS
3.19/3.18	20/30	LS	2.90/2.91	5/80	LC
3.11/3.14	12/12	LS	2.81/2.81	9/100	LC
2.91/2.91	5/80	LC	2.79/2.79	12/10	LS
2.81/2.81	8/100	LC	2.47/2.47	20/20	LS
2.79/2.79	11/10	LS	1.95/1.94	8/10	LS
2.62/2.62	9/30	LC	1.87/1.87	6/6	LS
2.47/2.47	20/20	LS	1.49/1.49	4/4	LS

Note. RbS is Rb_2SO_4.

TABLE IV

LATTICE CELL CONSTANTS OF PURE Li_2SO_4 (UNQUENCHED AND QUENCHED) AND Li_2SO_4 BELONGING TO DOPED EUTECTIC SYSTEMS

Sr. no.	Composition	a	b	c
1	Standard[a]	8.242	4.954	8.471
2	Unquenched	8.242	4.955	8.470
3	Quenched	8.243	4.970	8.466
4	Eut. + 1.5 mole% Na_2SO_4	8.244	4.957	8.477
5	Eut. + 1.5 mole% K_2SO_4	8.243	4.959	8.479
6	Eut. + 1.5 mole% Rb_2SO_4	8.244	4.959	8.480

[a] ASTM card no. 20-639A.

is observed. An anisotropic expansion of Li_2SO_4 has also been seen by Mellander and Nilsson (*10*). On the other hand, for 3 and 5 mole% of Na_2SO_4 and K_2SO_4 a close agreement between the observed and JCPDS values is found for $LiNaSO_4$ and $LiKSO_4$, along with Li_2SO_4 and Li_2CO_3 (Tables I and II).

In case of Rb_2SO_4, no phase corresponding to $LiRbSO_4$ forms. As a result of this, Rb_2SO_4 precipitates away, which is confirmed from XRD data given in Table III. However, as a result of the formation of multiphase materials in each case, the experimental and JCPDS values of the relative intensities (I/I_0) of the respective phases differ significantly.

In the present case, it is very interesting to note the presence of $LiNaSO_4$ and $LiKSO_4$, and the absence of $LiRbSO_4$; this is due to the possible contribution made by Li_2CO_3. The formation of intermediate compounds has also been observed in the LiI–NH_4I (*11*) and LiI–Li_3N–LiOH–Al_2O_3 (*12*) systems.

From detailed analysis of X-ray diffraction data, it is clear that the composite materials under investigation fulfill the essential condition for eutectic formation, i.e., that the individual phase present in the sample has limited solid solubility, and each species has a strong preference for its own crystal structure.

The bulk conductivity, obtained from impedance analysis discussed elsewhere (*9*), is plotted as a function of Na_2SO_4 concentration at 473 K in Fig. 1. It can be clearly seen that there are two conductivity maxima at 0.1 and 5.0 mole % of Na_2SO_4. Similar results are observed for the eutectic with K_2SO_4. But, for the eutectic with Rb_2SO_4 added there is only one maximum in the conductivity isotherm. In order to explain the conductivity results, the entire compositional range is divided into two regions: (I) from 0 to 2.0 mole% of Me_2SO_4 and (II) from 2.0 to 8.0 mole% of Me_2SO_4.

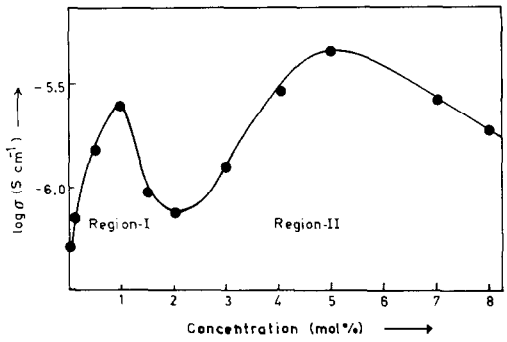

FIG. 1. Variation of log σ versus concentration of Na_2SO_4 in Li_2SO_4 : Li_2CO_3 eutectic at 453 K.

Ionic Conductivity in Region-I

Figure 2 illustrates the variation of log σT versus $10^3/T$ for Na_2SO_4 added eutectic system. From this figure it is evident that the conductivity of these samples obeys the Arrhenius relationship.

$$\sigma T = (\sigma T)_0 e^{(-\Delta E/kT)} \qquad (1)$$

in the entire temperature range of investigation. From the inset of the figure it is also

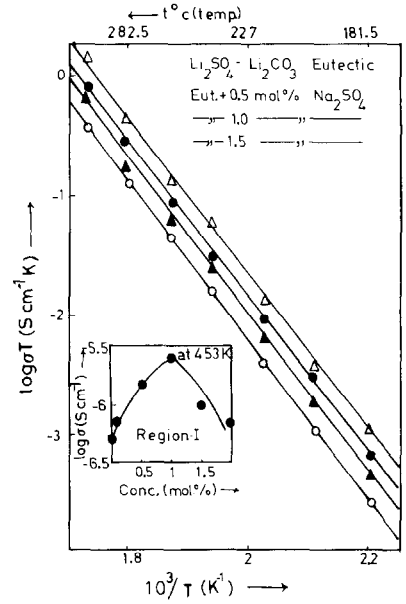

FIG. 2. Variation of log σT versus $10^3/T$ for Na_2SO_4 added Li_2SO_4 : Li_2CO_3 eutectic.

seen that the conductivity increases with increased Na_2SO_4 concentration. It exhibits a maximum at 1 mole% and decreases thereafter. The conductivity results for K_2SO_4 and Rb_2SO_4 doped eutectic show a similar behavior (Figs. 3 and 4).

Since for Me_2SO_4 doped eutectic systems, the anions and the cations of the host and guest materials are of same valency, the enhancement in conductivity for the above systems cannot be explained by the classical theory of aliovalent doping (*13*). Obviously, the main factor responsible for an enhancement in σ in this case is considered to be lattice distortions (elastic displacement) caused by the incorporation of the bigger guest ion into the host lattice. Because of such distortion, the lattice is forced to expand and undergoes a strain which depends on the value of

$$|1 - r_g/r_h|,$$

where r_g and r_h are the ionic radii of the guest and host ions, respectively. The net result of such strain is apparently lattice loosening leading to a decrease in melting point of the material. This is substantiated by the experimental results (Fig. 5), where the melting point decreases with the increase in ionic size of the impurity ion. Shahi and Wagner (*14*) have also observed similar results in case of AgBr–AgI mixed crystals.

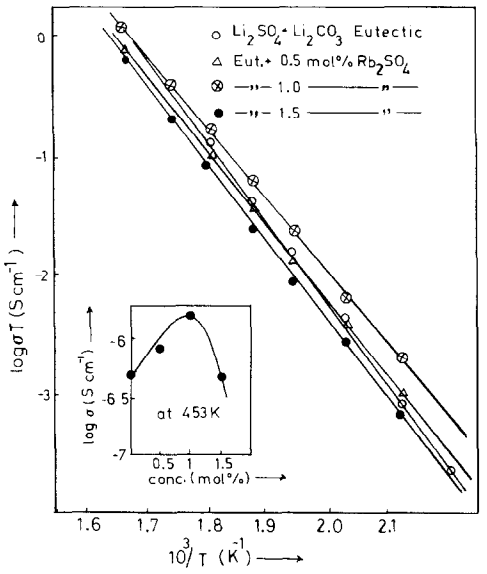

FIG. 3. Variation of log σT versus $10^3/T$ for K_2SO_4 added Li_2SO_4 : Li_2CO_3 eutectic.

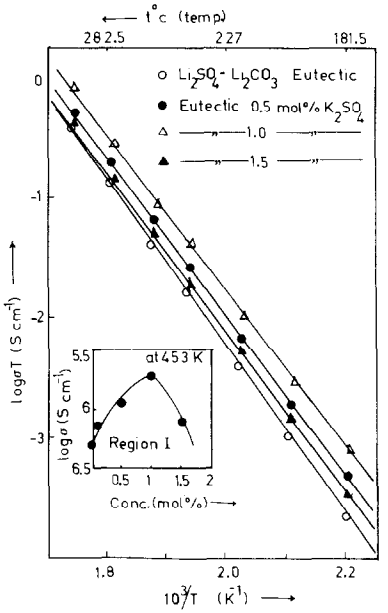

FIG. 4. Variation of log σT versus $10^3/T$ for Rb_2SO_4 added Li_2SO_4 : Li_2CO_3 eutectic.

The model based on the mobility of the ions as a function of lattice distortion leads to the several structural interpretations. In the simplest case there are no obstructions to the mobile Li^+ due to the presence of bigger Me^+, which, in turn, gives rise to a linear relationship between the conductivity and the degree of lattice distortion. This can only be expected at low dopant concentrations (0.5 to 1 mole%). But at its high concentrations, when the obstructions are predominent, the situation becomes more complicated.

The above process can also be visualized by considering a plane of host matrix as shown schematically in Fig. 5a. Here, the

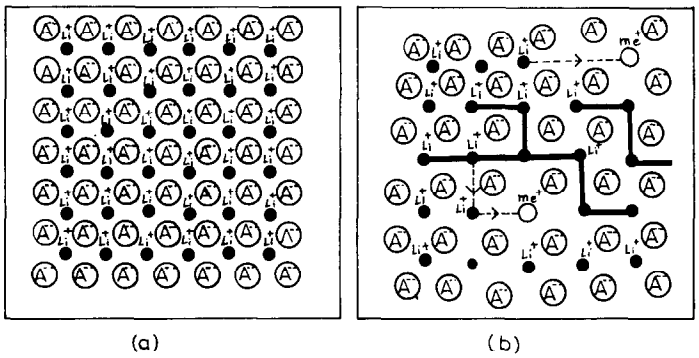

FIG. 5. Schematic representation of (a) plane through the lattice of host and (b) host lattice in which Li^+ sites are randomly occupied by relatively large size Me^+, resulting into the local distortion in the lattice. The thick lines indicate the percolating pathways created due to the local expansion in the lattice, and dashed lines show the obstruction caused by bigger Me^+.

dopant Me^+ is substituted randomly for Li^+. Although Me^+ and Li^+ possess the same charge, there is a large difference in their ionic sizes. Therefore, the partial replacement of the former for the latter produces the elastic distortion (local lattice expansion) in the host lattice (Fig. 5b). Such lattice distortion opens the lattice structure and, in turn, gives rise to a large number of interconnecting pathways between the adjacent interstitial sites (shown by thick lines) through which the Li ions percolate easily. Such percolating pathways increase linearly with increasing dopant concentration. At the same time, the bigger size of the guest ions offers a great energy barrier (obstruction) to the mobile Li^+ (as shown by the dotted lines). For very low dopant concentrations, however, such obstruction is negligible, but at higher concentrations it predominates, leading to a decrease in percolating pathways and hence the conductivity. The conductivity maximum at 1 mole% of Me_2SO_4 is attributed to the percolation threshold concentration.

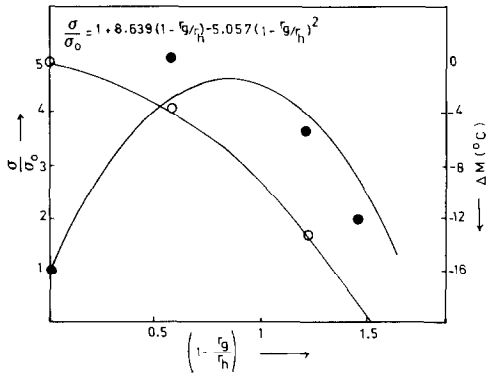

FIG. 6. Variation of normalized conductivity and decrease in melting point (ΔM) with change in relative ionic radii of dopant.

Figure 6 depicts the variation of conductivity and decrease in melting point (T_m) as a function of normalized ionic radius, which can also be described by following the empirical relation

$$\sigma/\sigma_0 \sim 1 + 8.636\,|1 - r_g/r_h| - 5.057\,|1 - r_g/r_h|^2.$$

It is worth noting here that maximum conductivity is observed for a particular guest ion having ionic radius = 1.11 Å (obtained from the above relation), though the melting point of the samples decreases continuously with increasing ionic radius of the dopant. These results substantiate the proposed model and suggest that the obstruction caused by the bigger guest ion to the mobile ions also plays an important role.

TABLE V

THE ELECTRICAL CONDUCTIVITY DATA FOR Me_2SO_4 (Me = Na, K, AND Rb) ADDED EUTECTIC

Compositions	ΔE (eV)	$(\sigma T)_0$ (S cm^{-1} K)	σ at 463 K (S cm^{-1})
		Eutectic	
	1.09	6.84×10^8	2.04×10^{-6}
		Eut. + Na_2SO_4	
Eut. + 3 mole%	1.05	5.84×10^8	2.72×10^{-6}
Eut. + 5 mole%	0.88	1.59×10^7	9.11×10^{-6}
Eut. + 8 mole%	1.04	4.13×10^8	4.31×10^{-6}
		Eutectic + K_2SO_4	
Eut. + 3 mole%	1.09	7.12×10^8	2.13×10^{-6}
Eut. + 5 mole%	0.98	1.03×10^8	4.84×10^{-6}
Eut. + 8 mole%	1.03	1.92×10^8	2.57×10^{-6}
		Eutectic + Rb_2SO_4	
Eut. + 3 mole%	1.08	2.38×10^8	9.11×10^{-7}
Eut. + 5 mole%	1.07	4.65×10^7	2.29×10^{-7}

Ionic Conductivity in Region-II

The conductivity of 3, 4, 5, 7, and 8 mole% of the eutectic with Me_2SO_4 added obeys the Arrhenius law (Eq. (1)). From this equation σ at 463 K, $(\sigma T)_0$ and ΔE are determined. From the results presented in Table V, it can be seen that the conductivity of the eutectic increases with increase in Me_2SO_4 (Me = Na and K) concentration. It attains a maximum at 5 mole% and decreases thereafter. On the other hand, conductivity decreases continuously with increased Rb_2SO_4 concentration in the eutectic. It is also interesting to note that the variation in activation energy and conductivity with concentration behaves exactly oppositely, and the minimum of the former coincides with the maximum of the latter. These results are comparable with those of the LKCN–γ–Al_2O_3 (*15*) and glass dispersed Li_2SO_4 : Li_2CO_3 eutectic composite solid electrolyte systems (*9, 16*). A similar enhancement in the conductivity due to the presence of an intermediate phase has been observed in the LiI–NH_4I (*11*), LiI–LiOH–Al_2O_3 (*17*), and LiI–Li_3N–LiOH–Al_2O_3 (*12*) systems.

Figures 7a and b display microphotographs of 5 and 8 mole% of Na_2SO_4 added eutectic, respectively. From these figures it is clear that, for low Na_2SO_4 concentrations, the intermediate $LiNaSO_4$ phase is dispersed uniformly throughout the sample, whereas the grains of $LiNaSO_4$ agglomerate at higher concentrations. The agglomeration of the grains disturbs the finely distributed nature of the eutectic and also creates the voids in the sample. In case of eutectic with K_2SO_4 added a similar result is observed.

The models developed so far in the area of composite solid electrolyte systems are limited to (a) polycrystalline materials (*MX/MX*) (*18*), (b) conducting–conducting (*MX/MX'*) (*19*), and (c) conducting–nonconducting (*MX/A*) systems (*20*). The present system is a bit different than these three systems because of its three ionically conducting constituents, namely (i) Li_2SO_4ss (solid solution of Li_2SO_4 with Me_2SO_4), (ii) Li_2CO_3, and (iii) $LiMeSO_4$. Thus, the total conductivity in the present system is considered to be due to the contributions from (i) Li_2SO_4ss, (ii) Li_2CO_3, (iii) $LiMeSO_4$, and (iv) the interface region between these phases. Since the observed conductivity is much higher than each of the individual phases present therein, an enhancement in the conductivity is due to the increase in concentration of the charge carriers (ions or vacancies) forming a diffuse space charge layer (*21*) or the enhancement in the ionic mobility in or near the interface due to the more distorted structure (*22*). The applicability of the former mechanism to the present system is more appropriate than the latter. The formation of a space charge layer at different interfaces is as follows: (a) at the interface of Li_2SO_4ss–Li_2SO_4ss, Li_2CO_3–Li_2CO_3, and $LiMeSO_4$–$LiMeSO_4$ it is similar to that as in case of *MX/MX* (*18*) and (b) at the interface between two ionically conducting phases it is equivalent to that of *MX/MX'* (*19*).

At the interface of two ion conductors (*MX/MX'*), the transport of the ions is not

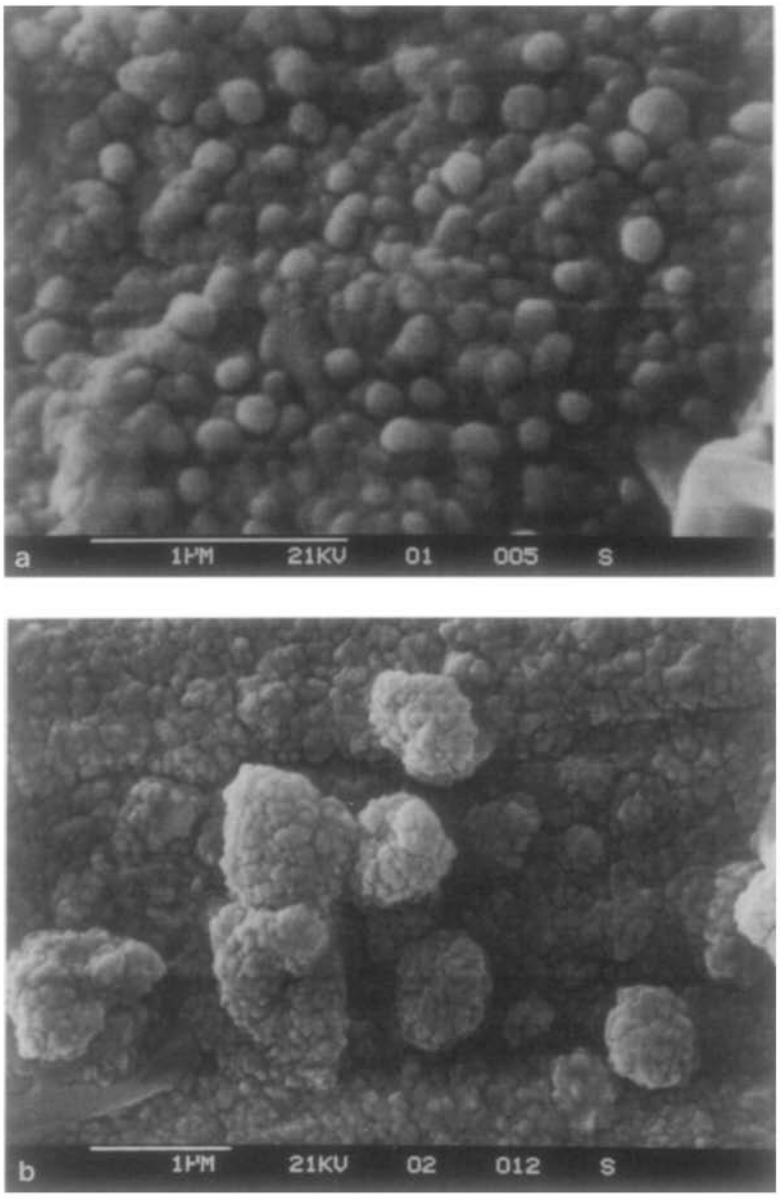

FIG. 7. Microstructures of (a) Li_2SO_4 : Li_2CO_3 eutectic + 5 mole% Na_2SO_4 and (b) Li_2SO_4 : Li_2CO_3 eutectic + 8 mole% Na_2SO_4.

only parallel to the interface, but an additional contribution comes from an interface with the other conductor, i.e., net transfer of ions from *MX* to *MX'* is also favorable (*23*). Therefore, in the present case, the conductivity across the grain boundaries is also of equal importance.

Conclusion

The solid solubility of Me_2SO_4 in Li_2SO_4 : Li_2CO_3 eutectic is less than 2 mole%. At higher concentrations (>2 mole%), they react with the Li_2SO_4 and form the intermediate phases $LiMeSO_4$ (*Me* = Na and K), which later get distributed throughout the

eutectic. The two conductivity maxima, one at 1 mole% and other at 5 mole% result from lattice distortion and dispersion of intermediate phases, respectively.

The maximum conducting sample (5 mole% of Na_2SO_4 added eutectic) can be used in the appropriate electrochemical devices.

The optimization of ionic conductivity in solid electrolyte system by the dispersion of second insoluble conducting phase may constitute a better strategy in materials research. Moreover, it complements the established approaches: doping, stabilization of highly conducting phases, building of new compounds, and dissolution of ionic salts in polymer and glasses.

References

1. C. C. LIANG, *J. Electrochem. Soc.* **120,** 1289 (1973).
2. F. W. POULSEN, *in* "Proceedings, 6th International Symposium" (F. W. Poulsen, N. H. Andersen, K. Clausen, S. Skaarup, and O. T. Sorensen, Eds.), p. 67, GH-Tryk I/S_1 Odense, Denmark (1985).
3. M. AMODORI, *A. Hi. R. Accad. Naz. Lincei, Sez, II,* **21,** 65 (1912).
4. M. A. K. L. DISSANAYAKE AND B. E. MELLANDER, *Solid State Ionics* **21,** 279 (1986).
5. V. K. DESHPANDE AND K. SINGH, *J. Power Sources* **10,** 191 (1983).
6. V. K. DESHPANDE AND K. SINGH, *Solid State Ionics* **8,** 319 (1983).
7. S. S. BHOGA AND K. SINGH, *Solid State Ionics* **40/41,** 27 (1990).
8. K. SINGH, S. S. BHOGA, AND V. K. DESHPANDE, *in* "Current Trends in Physics of Materials" (M. Youssouf, Ed.), p. 228. World Sci, Singapore (1986).
9. K. SINGH AND S. S. BHOGA, *J. Electrochem. Soc.* **137,** 1970 (1990).
10. B. E. MELLANDER AND L. NILSSON, *Z. Naturforsch.* **38a,** 1396 (1983).
11. P. HARTWIG AND W. WEPPNER, *Solid State Ionics* **5,** 403 (1981).
12. P. HARTWIG, W. WEPPNER, AND W. WICHELHAUS, *Mater. Res. Bull.* **14,** 493 (1979).
13. H. H. HOFER, W. EYSEL, AND U. VON ALPEN, *J. Solid State Chem.* **36,** 365 (1981).
14. K. SHAHI AND J. B. WAGNER, JR., *J. Phys. Chem. Solids* **43,** 713 (1982).
15. C. LIQUAN, *in* "Materials for Solid State Batteries" (B. V. R. Chowderi and S. Radhakrishna, Eds.), p. 9. World Sci, Singapore (1986).
16. K. SINGH AND S. S. BHOGA, *Solid State Ionics* 40 (1990).
17. P. HARTWIG AND W. WEPPNER, *Solid State Ionics* **3/4,** 249 (1981).
18. J. MAIER, *Ber. Bunsenges. Phys. Chem. Solids* **90,** 29 (1986).
19. J. MAIER, *Ber. Bunsenges. Phys. Chem. Solids* **89,** 355 (1985).
20. J. MAIER, *J. Phys. Chem. Solids* **46,** 309 (1985).
21. J. B. PHIPS AND D. H. WHITMORE, *Solid State Ionics* **9/10,** 123 (1983).
22. A. K. SHUKLA, N. VAIDEHI, AND K. T. JACOB, *Proc. Indian Acad. Sci. Chem. Sci.* **96,** 533 (1986).
23. J. MAIER, *Ber. Bunsenges. Phys. Chem. Solids* **88,** 1057 (1984).